Chalcogenide Letters Vol. 17, No. 10, October 2020, p. 529 - 536

# CdS/CdSe HETEROSTRUCTURES GROWN BY CHEMICAL TECHNIQUES ON FLEXIBLE PET/ITO SUBSTRATES

K. RODRÍGUEZ-ROSALES[a], K. NIETO-ZEPEDA[a,*],
J. G. QUIÑONES-GALVÁN[b], J. SANTOS-CRUZ[a],
S. A. MAYÉN-HERNÁNDEZ[a], A. GUILLEN-CERVANTES[c],
F. DE MOURE-FLORES[a]
[a]*Faculty of Chemistry, Materials-Energy, Autonomous University of Querétaro (UAQ), C.P. 76010 Santiago de Querétaro, Qro, México*
[b]*Department of Physics, University Center for Exact Sciences and Engineering, Guadalajara University, Guadalajara, Jalisco, C.P. 44430, México.*
[c]*Department of Physics, CINVESTAV-IPN, Apdo. Postal 14-740, México D. F. 07360, México*

Undoped and Mn-doped CdS films, CdSe films and CdS:Mn/CdSe heterostructures were deposited by chemical techniques. Undoped and Mn-doped CdS films were grown onto flexible PET/ITO substrates by chemical bath deposition at different temperatures. CdSe thin films were synthesized following a two stages process. In the first stage, $CdO_2$ precursor films, were synthesized by chemical bath deposition at different deposition time. In the second stage, the $CdO_2$ precursor films were transformed into CdSe films by immersion in a Se ionic solution. CdS, CdS:Mn, CdSe and CdS/CdSe samples were characterized by high-resolution transmission electron microscopy, UV-vis, Raman and room temperature photoluminescence spectroscopies. The structural characterization indicates that CdS and CdSe films with hexagonal phase were obtained. CdSe films showed the LO Raman mode with three order phonon replicas, an indication of the excellent crystalline quality of the samples.

(Received August 5, 2020; Accepted October 28, 2020)

*Keywords:* CdS films, CdSe films, CdS/CdSe heterostructure, Chemical bath deposition, Mn-doping

## 1. Introduction

II-VI semiconductor compounds are important for scientific and technological applications due to their physical properties [1-3]. The CdS and CdSe compounds can crystallize in two structures: cubic (zinc blende) and hexagonal (wurtzite). CdS and CdSe have a direct band gap of 2.42 eV and 1.70 eV, respectively [4-6]. Polycrystalline thin films of both can be deposited by several techniques such as chemical bath deposition (CBD) [7,8], electrodeposition [1,9,10], vacuum evaporation [11,12], molecular beam epitaxy [13,14], magnetron sputtering [15,16], among others [9,17-19]. The physical techniques require complex equipment, which translates into high costs. The chemical synthesis is very attractive due to its feasibility to produce large-area thin films at low cost [20]. The quality of semiconductor films deposited by chemical synthesis depends on growth parameters such as precursor concentrations and pH and temperature of the solution.

Over the last years, flexible substrates have demonstrated great potential to be used in flexible displays, flexible organic light-emitting diodes, and flexible solar cells [21,22]. Particularly, polyethylene terephthalate (PET) substrate has been used for photovoltaic devices because of its high optical transmission in the visible region, low cost, good flexibility and lightweight [23,24]. In this work, we report the fabrication of the CdS:Mn/CdSe heterostructure by chemical techniques on flexible PET/ITO substrates.

* Corresponding author: karen_1704@hotmail.com

## 2. Experimental details

### 2.1 Growth of thins films

Undoped and Mn-doped CdS films were deposited on PET/ITO substrates with a size of 2.5 x 2.0 $cm^2$ by CBD at different temperatures. The reaction solution was prepared mixing 0.025 M $CdCl_2$, 0.075 M $NH_4Cl$, 0.05 M $((NH_2))_2CS$), 1.56 μM $Mn(C_2H_3O_2)_2$. $CdCl_2$ and $((NH_2))_2CS$) were employed as cadmium and sulfur sources, respectively. $NH_4Cl$ had the function of complexing the reaction process and keeping the pH at 11. $Mn(C_2H_3O_2)_2$ was employed as an Mn dopant source. The undoped and Mn-doped CdS films were grown by 180 minutes at bath temperatures of 70 °C, 80 °C and 90 °C.

CdSe samples were synthesized in two stages. In the first stage, $CdO_2$ films were prepared by CBD on PET/ITO or PET/ITO/CdS substrates at 50 ºC and 10 minutes, the details of $CdO_2$ films deposition are described in reference [9]. In the second stage, the $CdO_2$ films were immersed in a selenium solution for 5 minutes to transform $CdO_2$ films into CdSe. The Se ionic solution was prepared in a beaker containing deionized water, 4 g of sodium hydroxide (NaOH), 5 g of hidroximetanosulfunic acid ($CH_3NaO_3S \cdot 2H_2O$), and 5 g of elemental Se. The components were heated to 70 ºC under magnetic stirring for 15 minutes. After immersion, CdSe samples were rinsed in distilled water and dried with nitrogen gas.

### 2.3. Characterization

Samples were structurally characterized by High-Resolution Transmission Electron Microscopy (HR-TEM) using a JEOL JEM 2010 microscope with a lanthanum hexaboride filament at an acceleration voltage of 200 kV. The optical properties were determined by UV-Vis and room temperature photoluminescence (RT-PL) spectroscopies. The optical transmittance spectra were obtained with a Perkin-Elmer Lambda-2 spectrophotometer, while PL spectra were obtained at room temperature using an Omnichrome-Series56 He-Cd laser with the 325 nm line. Raman measurements were achieved through a micro-Raman spectrometer (Jobin Yvon, model Labram) using the 632.8 nm line from He-Ne laser.

## 3. Results and discussion

### 3.1. Undoped and Mn-doped CdS films

HR-TEM micrographs of undoped and Mn-doped CdS films grown at different temperatures by CBD are shown in Fig. 1 and Fig. 2, respectively. Undoped CdS films grown at 70 °C and 80 °C have crystals with hexagonal phase-oriented in the (100) and (110) directions, respectively. The undoped CdS sample grown at 90 °C presents crystals with the orientation (200) of the cubic phase. Mn-doped only presents crystals with hexagonal phase orientated in the (101) direction. This indicates that the Mn-doped promotes the formation of the hexagonal phase.

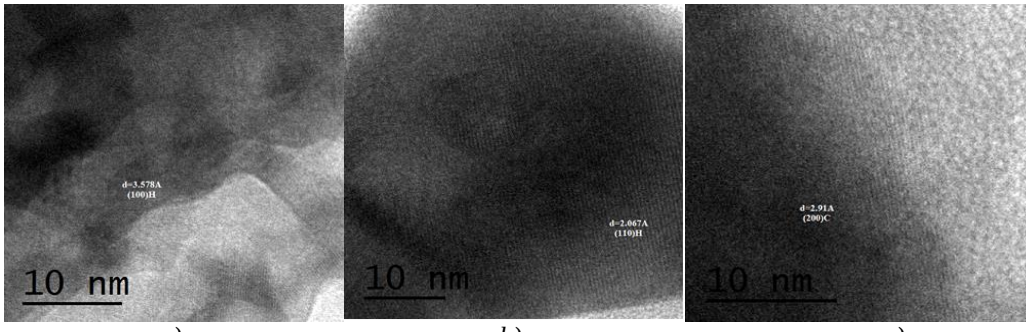


*a)* *b)* *c)*

*Fig. 1. HR-TEM images of undoped CdS films grown on PET/ITO substrates at different temperatures: a) 70 ºC, b) 80 ºC y c) 90 ºC.*

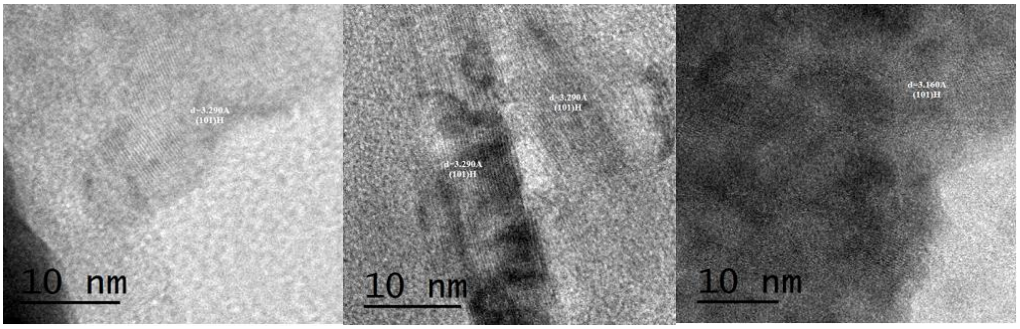


*a)* *b)* *c)*

*Fig. 2. HR-TEM images for Mn-doped CdS films grown PET/ITO substrates at different temperatures: a) 70 ºC, b) 80 ºC y c) 90 ºC.*

Optical properties of CdS films were analyzed by both UV-Vis and photoluminescence spectroscopies. The optical transmittance spectra of undoped CdS films are shown in Fig. 3a). The undoped CdS films have a transmittance between 65% and 70% in the visible range of the electromagnetic spectrum. The transmittance spectra of Mn-doped CdS films are shown in Fig. 4a). Mn-doped CdS films have a transmittance between 60-80%. The absorption coefficient was calculated by the relation $T = (1 - R)^2 \exp(-\alpha d)$, where T is the transmittance, R is the reflectance and *d* the film thickness. The absorption coefficient was used to determine the band gap ($E_g$) of undoped and Mn-doped CdS films using the Tauc approximation; $\alpha h\nu = (h\nu - E_g)^{1/2}$, where $h\nu$ is the photon energy [25]. The $E_g$ was determined by fitting the linear part of the curve, as shown in Fig. 3b) and 4b). Undoped CdS samples grown at 70 °C, 80 °C and 90 °C have an $E_g$ of 2.32 eV, 2.27 eV and 2.30 eV, respectively. In general, the $E_g$ value decreases when the growth temperature rises. The CdS:Mn-70 sample has an $E_g$ value of 2.23 eV, whereas CdS:Mn-80 and CdS:Mn-90 samples have a band gap value of 2.27 eV. The band gap values for Mn-doped CdS films decrease with respect to undoped CdS films; donors induce energy levels inside the $E_g$ of CdS extending the conduction band into the band gap, reducing the energy edge of CdS:Mn samples [26].

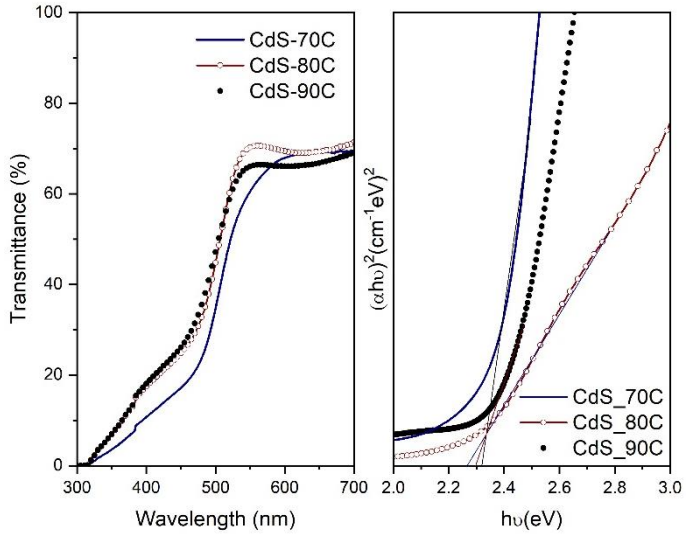


*a* *b)*

*Fig. 3. a) Optical transmittance spectra of undoped CdS films deposited at different temperatures, b) Band gap calculations for undoped CdS films deposited at different temperatures.*

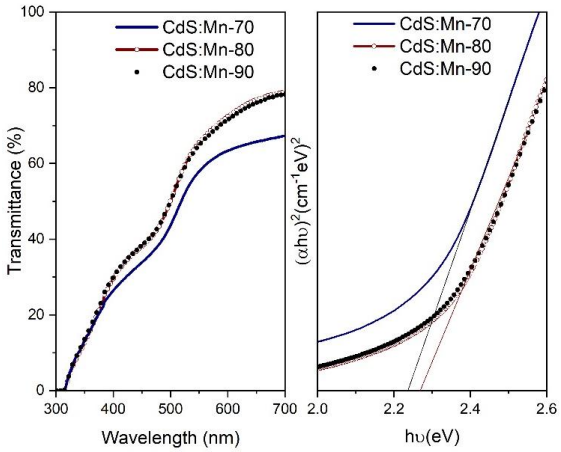


*Fig. 4. a) Optical transmittance spectra of Mn-doped CdS films deposited at different temperatures, b) Band gap calculations for Mn-doped CdS films deposited at different temperatures.*

Fig. 5 shows the room temperature PL spectra of Mn-doped CdS films grown at different temperatures by CBD on PET/ITO substrates. Mn-doped CdS have the green emission at 2.31-2.37 eV. A signal centered at 3 eV can be seen for samples grown at 70 and 80 °C; this band is associated with the PET/ITO substrate [27]. Spectrum for the sample grown at 90 °C presents a shoulder at 3 eV along with a strong band centered at 2.8 eV. The signal at 3 eV corresponds to the substrate. In reference [27], it was found that CdS nano-crystals have an emission at 2.8 eV, thus the signal observed in figure 5 for the sample grown at 90 °C is associated with the presence of CdS nano-crystals. Spectra for samples deposited at 70 and 80 °C have this signal as a shoulder. The green band has its origin in radiative transitions from donor levels to the top of the valence band, which may be due to states generated by interstitial cadmium ($Cd_i$) [28].

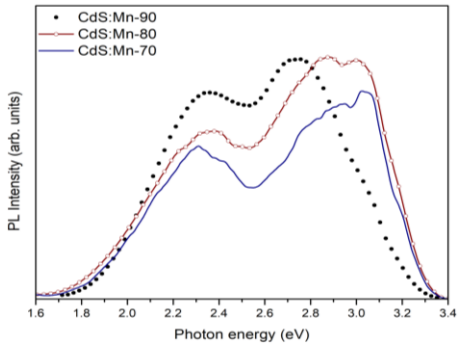


*Fig. 5. Photoluminescence spectra of Mn-doped CdS films grown by CBD at different temperatures: 70 °C, 80 °C and 90 °C.*

### 3.2 CdSe thin films and CdS:Mn/CdSe heterostructures

The Raman spectra of CdSe films grown by chemical synthesis on PET/ITO and PET/ITO/CdS:Mn substrates are shown in Fig. 6. All spectra showed the CdSe longitudinal optical (1LO) mode at a frequency of 207 $cm^{-1}$, the second (2LO) and third (3LO) modes, characteristic of CdSe [12], appear at 414 $cm^{-1}$ and 621 $cm^{-1}$, respectively. The appearance of 2LO and 3LO modes is an indication of the high crystalline quality of the CdSe films. For CdSe, these modes are a consequence of the stretching $Cd^{2+}$ and $Se^{2-}$ ions [29]. The observed 1LO mode is slightly shifted to a lower frequency with respect to the 1LO mode for bulk CdSe, this Raman shift in the LO

modes may be due to the nanocrystalline nature and/or strain effects in CdSe films [17]. Fig. 7 shows the HR-TEM image of a CdSe thin film grown by chemical synthesis on the Mn-doped CdS substrate obtained at 90 °C (PET/ITO/CdS:Mn-90C sample). The presence of nano-crystals with the (101) orientation of the hexagonal CdSe phase can be observed, which is in agreement with Raman analyzes.

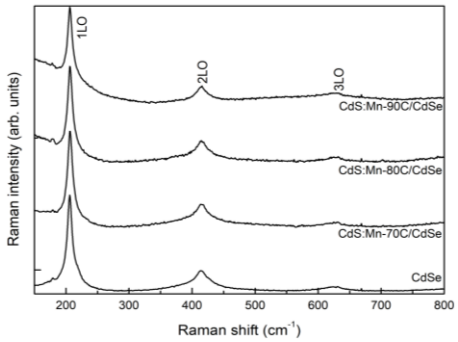


*Fig. 6. Raman spectra of CdSe thin films grown by chemical synthesis on PET/ITO/CdS:Mn substrates. Mn-doped CdS films were deposited by CBD at different temperatures: 70 °C, 80 °C and 90 °C.*

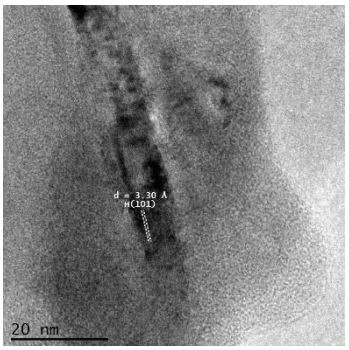


*Fig. 7. HR-TEM micrograph of a CdSe film grown by chemical synthesis on a CdS:Mn film grown by CBD at 90 °C.*

In the same way, as for CdS films, the band gap was calculated from optical transmittance measurements. Fig. 8a) exhibits band gap calculations for CdSe thin films grown by chemical synthesis on PET/ITO substrates during 1.0 h and 1.5 h, the CdSe-1.0h film has an $E_g$ of 1.69 eV, while the CdSe-1.5h sample has an $E_g$ of 1.66 eV. These band gap values are close to 1.70 eV reported for CdSe [30]. Band gap calculations for CdSe films grown on CdS:Mn substrates are shown in Fig. 8b). The $E_g$ values of CdSe films are between 1.60-1.66 eV. Fig. 9 shows the room temperature PL spectra of CdSe thin films grown by chemical synthesis on PET/ITO and PET/ITO/CdS:Mn substrates. All spectra show four signals, with different intensity, located at 1.55 eV, 2.0-2.20 eV, 2.33-2.40, and a shoulder at 2.9-3.0 eV. The band at 1.55 eV corresponds to CdSe nanoparticles [9], in agreement with the observed in HR-TEM. The signal at 2.0-2.20 eV corresponds to the $SeO_2$ compound [9], which is a precursor for the formation of the CdSe film. For CdSe films grown on PET/ITO/CdS:Mn substrates the intensity signals decreases considerably except for the sample in which the CdS:Mn was obtained at 90 °C (PET/ITO/CdS:Mn-90/CdSe sample), this indicates that the CdS:Mn film (substrate) grown at 90 °C promotes the formation of the CdSe compound.

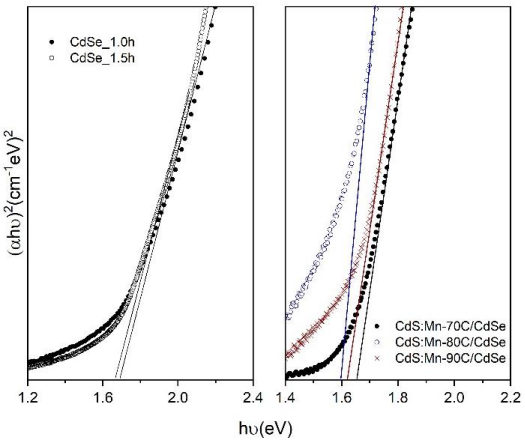


*Fig. 8. Band gap calculations for CdSe films grown by chemical synthesis on a) PET/ITO substrates and b) CdS:Mn substrates*

*a)* *b)*

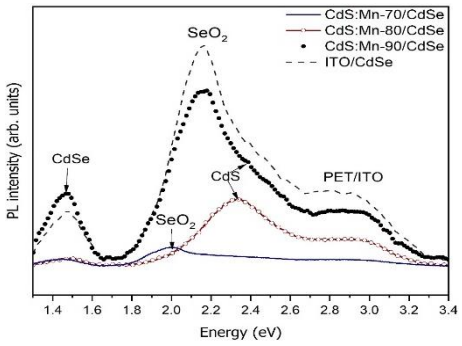


*Fig. 9. Photoluminescence spectra of a CdSe film and CdS:Mn/CdSe heterostructures.*

## 4. Conclusions

Undoped and Mn-doped CdS thins films were grown by chemical synthesis on PET/ITO substrates at different temperatures: 70 °C, 80 °C and 90 °C. The structural characterization (TEM) showed that undoped CdS films grown at 70 °C and 80 °C have a hexagonal phase, while the undoped CdS sample grown at 90 °C has a cubic phase. CdS:Mn films grown at different temperatures have the CdS hexagonal phase. The optical transmittance of undoped and Mn-doped films was found between 65-70% and 60-80% for wavelengths above 550 nm. The band gap values for Mn-doped CdS films decreases with respect to undoped CdS films. Raman and TEM characterization showed that CdSe films have a hexagonal phase. CdSe films have a ban gap between 1.66-1.67 eV; these values are close to 1.70 eV reported for CdSe. The photoluminescence spectra of the CdSe films showed an emission at 1.55 eV, characteristic of CdSe nanoparticles, which is in agreement with TEM analysis.

It has been demonstrated that a complete semiconductor heterostructure of the system CdS/CdSe can be achieved by chemical methods on PET/ITO substrates, which is promising for flexible optoelectronics applications.

**Acknowledgments**

We acknowledge the technical support of Marcela Guerrero, and A. García-Sotelo from the Physics Department of the CINVESTAV-IPN. The authors also acknowledge the financial support for this work from FONDO SECTORIAL CONACYT-SENER-SUSTENTABILIDAD

ENERGÉTICA through CeMIE-sol, within of the strategic project number 37: “Development of new photovoltaic devices and semi-superconductor materials”.

## References

[1] C. Lu, L. Zhang, Y. Zhang, S. Liu, G. Liu, Appl. Surf. Sci. **319**, 278 (2014).
[2] S. R. Alharbi, Mater. Sci. Semicond. Process. **76**, 1 (2018).
[3] M. Hassen, R. Riahi, F. Laatar, H. Ezzaouia, Surfaces and Interfaces **18**, 100408 (2020).
[4] P. M. P. Salomé, J. Keller, T. Törndahl, J. P. Teixeira, N. Nicoara, R. Andrade, D. G. Stroppa, J. C. González, M. Edoff, J. P. Leitão, S. Sadewasser, Sol. Energy Mater. Sol. Cells **159**, 272 (2017).
[5] A. M. Ali, Y. Yusoff, L. M. Ali, H. Misran, M. Akhtaruzzaman, M. A. Alghoul, K. Sopian, S. Radiman, N. Amin, Sol. Energy **173**, 120 (2018).
[6] S. L. Patel, Himanshu, Kaushalya, S. Chander, M. D. Kannan, M. S. Dhaka, J. Mater. Sci. Mater. Electron. **30**, 20840 (2019).
[7] F. Laatar, A. Harizi, A. Smida, M. Hassen, H. Ezzaouia, Mater. Res. Bull. **78**, 83 (2016).
[8] R. Olvera-Rivas, J. Santos Cruz, F. de Moure-Flores, S. A. Mayén-Hernández, J. Quiñones-Galván, A. Centeno, A. Sosa-Domínguez, Chalcogenide Lett. **17**(7), 329 (2020).
[9] E. Lifshitz, I. Dag, G. Litvin, G. Hodes, S. Gorer, R. Reisfeld, M. Zelner, H. Minti, Chem. Phys. Lett. **288**, 188 (1998).
[10] S. Z. Werta, O. K. Echendu, F. B. Dejene, ECS J. Solid State Sci. Technol. **8**(2), P112 (2019).
[11] S. Aksu, E. Bacaksiz, M. Parlak, S. Yilmaz, I. Polat, M. Altunba, M. Türksoy, R. Topkaya, K. Özdoan, Mater. Chem. Phys. **130**(1-2), 340 (2011).
[12] N. S. Babu, M. A. Khadar, Sol. Energy Mater. Sol. Cells **178**, 106 (2018).
[13] J. W. Choi, A. Bhupathiraju, M. A. Hasan, J. M. Lannon, J. Cryst. Growth **255**(1-2), 1 (2003).
[14] Q. Yang, J. Zhao, M. Guan, C. Liu, L. Cui, D. Han, Y. Zeng, Appl. Surf. Sci. **257**(21), 9038 (2011).
[15] O. Toma, L. Ion, S. Iftimie, A. Radu, S. Antohe, Mater. Des. **100**, 198 (2016).
[16] C. Li, F. Wang, Y. Chen, L. Wu, J. Zhang, W. Li, X. He, B. Li, L. Feng, Mater. Sci. Semicond. Process. **83**, 89 (2018).
[17] R. B. Kale, S. D. Sartale, B. K. Chougule, C. D. Lokhande, Semicond. Sci. Technol. **19**(8), 980 (2004).
[18] J. Han, Y. Jian, Y. He, Y. Liu, X. Xiong, L. Cha, V. Krishnakumar, Mater. Lett. **177**, 5 (2016).
[19] K. B. Chaudhari, N. M. Gosavi, N. G. Deshpande, S. R. Gosavi, J. Sci. Adv. Mater. Devices **1**(4), 476 (2016).
[20] K. E. Nieto-Zepeda, A. Guillén-Cervantes, K. Rodríguez-Rosales, J. Santos-Cruz, D. Santos-Cruz, M. de la, O. Zelaya-Ángel, J. Santoyo-Salazar, L. A. Hernández-Hernández, G. Contreras-Puente, F. de Moure-Flores, Results Phys. **7**, 1971 (2017).
[21] L. La, P. Cataldi, L. Ceseracciu, I. S. Bayer, A. Athanassiou, S. Marras, E. Villari, F. Brunetti, A. Reale, Mater. Today Energy **7**, 105 (2018).
[22] P. E. Rodríguez-Hernández, J. G. Quiñones-Galván, L. Marasamy, M. Morales-Luna, J. Santos-Cruz, J. S. Arias-Cerón, O. Zelaya-Angel, F. de Moure-Flores, Mater. Sci. Semicond. Process. **103**, 104600 (2019).
[23] Y. H. Ko, M. S. Kim, J. S. Yu, Appl. Surf. Sci. **259**, 99 (2012).
[24] J. Jean, A. Wang, V. Bulovi, **31**, 120 (2016).
[25] S. L. Patel, A. Purohit, S. Chander, M. D. Kannan, M. S. Dhaka, Curr. Appl. Phys. **18**(7), 803 (2018).
[26] H. Khallaf, G. Chai, O. Lupan, L. Chow, S. Park, A. Schulte, J. Phys. D. Appl. Phys. **41**(18), (2008).
[27] K. Rodríguez-Rosales, J. G. Quiñones-Galván, A. Guillén-Cervantes, E. Campos-González, J. Santos-Cruz, S. A. Mayén-Hernández, J. S. Arias-Cerón, M. de la L. Olvera, O. Zelaya-Angel, L. A. Hernández-Hernández, G. Contreras-Puente, F. de Moure-Flores,

Mater. Res. Express **4**(7), 075904 (2017).
[28] A. E. Abken, D. P. Halliday, K. Durose, J. Appl. Phys. **105**(6), 064515 (2009).
[29] J. A. Rivera-Marquez, J. I. Contreras-Rascón, R. Lozada-Morales, J. Díaz-Reyes, R. Castillo-Palomera, M. E. Alvarez, M. Meléndez-Lira, O. Zelaya-Angel, Mater. Sci. Eng. B **260**, 114621 (2020).
[30] V. S. Raut, C. D. Lokhande, V. V. Killedar, J. Electroanal. Chem. **788**, 137 (2017).